



You have downloaded a document from  
**RE-BUŚ**  
repository of the University of Silesia in Katowice

**Title:** Effect of Sb and MnO<sub>2</sub>-Doping on Phase Transitions, Crystal Structure, Thermal, Dielectric, Ferroelectric and Piezoelectric Properties of Na<sub>0.5</sub>K<sub>0.5</sub>NbO<sub>3</sub> Ceramics

**Author:** J. Suchanicz, I. Faszczowy, P. Czaja, Joachim Kusz, Maciej Zubko

**Citation style:** Suchanicz J., Faszczowy I., Czaja P., Kusz Joachim, Zubko Maciej. (2018). Effect of Sb and MnO<sub>2</sub>-Doping on Phase Transitions, Crystal Structure, Thermal, Dielectric, Ferroelectric and Piezoelectric Properties of Na<sub>0.5</sub>K<sub>0.5</sub>NbO<sub>3</sub> Ceramics. "Archives of Metallurgy and Materials" (Vol. 63, iss. 2 (2018), s. 633-639), doi 10.24425/122387



Uznanie autorstwa - Użycie niekomercyjne - Bez utworów zależnych Polska - Licencja ta zezwala na rozpowszechnianie, przedstawianie i wykonywanie utworu jedynie w celach niekomercyjnych oraz pod warunkiem zachowania go w oryginalnej postaci (nie tworzenia utworów zależnych).



DOI: 10.24425/122387

J. SUCHANICZ<sup>#</sup>, I. FASZCZOWY\*, P. CZAJA\*, J. KUSZ\*\*, M. ZUBKO\*\*\*

**EFFECT OF Sb AND MnO<sub>2</sub>-DOPING ON PHASE TRANSITIONS, CRYSTAL STRUCTURE, THERMAL, DIELECTRIC, FERROELECTRIC AND PIEZOELECTRIC PROPERTIES OF Na<sub>0.5</sub>K<sub>0.5</sub>NbO<sub>3</sub> CERAMICS**

Lead-free ceramics of Na<sub>0.5</sub>K<sub>0.5</sub>Nb<sub>1-x</sub>Sb<sub>x</sub>O<sub>3</sub> (NKNS) and Na<sub>0.5</sub>K<sub>0.5</sub>Nb<sub>1-x</sub>Sb<sub>x</sub>O<sub>3</sub> + 0.5 mol%MnO<sub>2</sub> (NKNS + 0.5 mol%MnO<sub>2</sub>) (0 < x < 0.06) ceramics were prepared by a conventional solid-state hot pressing method. The ceramics possess a single-phase perovskite structure with orthorhombic symmetry. Microstructural examination revealed that Mn doping of NKNS leads to improvement of densification. The cubic-tetragonal and tetragonal-orthorhombic phase transitions of NKNS shifted to higher and lower temperature, respectively after introduction of Mn ion. Besides, ferroelectric and piezoelectric properties were improved. The results were discussed in term of difference in both ionic size and electronegativity of Nb<sup>5+</sup> and Sb<sup>5+</sup> and improvement of densification after Mn ion doping.

*Keywords:* Na<sub>0.5</sub>K<sub>0.5</sub>NbO<sub>3</sub>- based ceramics, structural properties, ferroelectric properties, dielectric properties, piezoelectric properties

### 1. Introduction

The lead-based ceramics have been widely used in sensors, actuators and transducers due to their excellent piezoelectric properties, and flexibility in term of compositional modifications. However, due to toxicity of the lead oxide (PbO) there is extensive research in lead-free ceramics.

Na<sub>0.5</sub>K<sub>0.5</sub>NbO<sub>3</sub> (NKN) and NKN-based compounds are considered as the most promising candidates as lead-free materials for replace lead-based ceramics [1,2]. However, pure and dense NKN ceramics is difficult to obtain by ordinary sintering process due to of the high volatility of alkaline elements under high sintering temperature. Evaporation of these elements degrades electric and piezoelectric properties. In order to improve density and consequently electric and piezoelectric properties of NKN and NKN-based ceramics additives were incorporated and other sintering processes were introduced.

In this study, the effect of Sb and 0.5 mol%MnO<sub>2</sub> on the crystal structure, phase transitions behaviour, thermal, dielectric, ferroelectric and piezoelectric properties of NKN ceramics obtained by solid state hot pressing sintering process were investigated.

### 2. Experimental details

The powders in stoichiometric ratio of Na<sub>0.5</sub>K<sub>0.5</sub>NbO<sub>3</sub> (NKN), Na<sub>0.5</sub>K<sub>0.5</sub>Nb<sub>1-x</sub>Sb<sub>x</sub>O<sub>3</sub> (NKNS) and Na<sub>0.5</sub>K<sub>0.5</sub>(Nb<sub>1-x</sub>Sb<sub>x</sub>)

O<sub>3</sub> + 0.5%MnO<sub>2</sub> (NKNS + 0.5mol%MnO<sub>2</sub>) were synthesized by solid state reaction from reagent grade oxides Nb<sub>2</sub>O<sub>5</sub> (99.9%), MnO<sub>2</sub> (99.9%) and carbonates Na<sub>2</sub>CO<sub>3</sub> (99.5%), K<sub>2</sub>CO<sub>3</sub> (99%). Before weighing, all starting powders were dried at 220°C for 2 days to remove any moisture and then stored in a desiccator for future use. The homogenization and grinding of raw materials were performed in an agate ball mill for 24 hours using anhydrous ethanol as the medium. The dried powders were calcinated twice at 880°C and 950°C for 5 h. After the calcination MnO<sub>2</sub> was added as a sintering aid and the powders were ball milled again. Then the dried powders were thoroughly mixed with 5wt% polyvinylalcohol (PVA) solution and uniaxially pressed into disc samples (diameter of 17 mm and 2-3 mm in thickness under 100 MPa pressure). The pellets were placed on a platinum foil, and the sintering was performed in a closed alumina crucible in air atmosphere at 1090-1140°C for 2-4 hours. The hot pressing of the samples was performed at 1100-1140°C for 2 hours under pressure of 25 MPa. After sintering, the samples were cooled with constant rate 150°C/h.

The microstructure was examined by scanning electron microscopy (Hitachi S-4700). The Electron Dispersive Spectroscopy (EDS) analysis was performed with Noran-Vantage system.

X-ray powder diffraction measurements were performed on Seifert powder diffractometer (XRD 3000 TT) with CuK $\alpha$  radiation at 45 kV and 30 mA in 2 $\theta$  range from 20 to 90°. High temperature powder measurements were performed also on Seifert powder diffractometer (XRD 3000 TT) with CuK $\alpha$  radiation at 45 kV and 30 mA equipped with high temperature attachment from

\* PEDAGOGICAL UNIVERSITY, INSTITUTE OF TECHNOLOGY, 2 PODCHORAZYCH STR., 30-084 KRAKOW, POLAND

\*\* UNIVERSITY OF SILESIA, INSTITUTE OF PHYSICS, 4 UNIWERSYTECKA STR., 40-007 KATOWICE, POLAND

\*\*\* UNIVERSITY OF SILESIA, INSTITUTE OF MATERIAL SCIENCE, 1A 75 PULKU PIECHOTY STR., 41-500 CHORZOW, POLAND

# Corresponding author: sfsuchan@up.krakow.pl

Materials Research Instruments. Measurements were performed during heating and cooling cycles with 15° and 5° temperature steps in  $2\theta$  range from 44 to 47.5° around (002)<sub>C</sub> diffraction peak clearly showing splitting during studied phase transitions.

For the evaluation of electrical properties silver paste electrodes were painted on both sides of the samples. The dielectric properties were measured with precision LCR meter GWINSTEK LCR-8110G. The heating/cooling rate of 4°C/min and frequency range of 0.1 kHz-1 MHz was used. Ferroelectric hysteresis loops were evaluated by a Sawyer-Tower circuit ( $f = 50$  Hz). The remanent polarization was obtained independently from pyroelectric measurements. The pyroelectric currents were recorded by using the Keithley 6517A electrometer by quasistatic method after polarising in dc electric fields of 12 kV/cm from 250°C to room temperature. Piezoelectric properties were measured by a resonance-antiresonance method on the basis of IEEE 176-1987 standards, using an impedance analyser (HP 419A).

The specific heat measurements were carried out using a Netzsch DSC F3 Maia scanning calorimeter in the temperature range from room temperature to 550°C under argon atmosphere at a flow rate 30 ml/min. The specimen consisted of single piece of sample of the average mass 20 mg was placed in an alumina crucible. The data were collected upon heating and cooling with a constant rate of 10°C/min.

The powders Raman spectra were recorded in Bio-Rad FTS 6000 spectrometer with Nd-Yag laser system, where the 1064 nm line was used as excitation line. The laser power was 200 mW. The spectra were collected with 4 cm<sup>-1</sup> resolution.

### 3. Results and discussion

Figure 1 shows the microstructure of investigated samples. It can be observed that all specimens have dense microstructure. With increase of Sb content grain size showed increasing trend

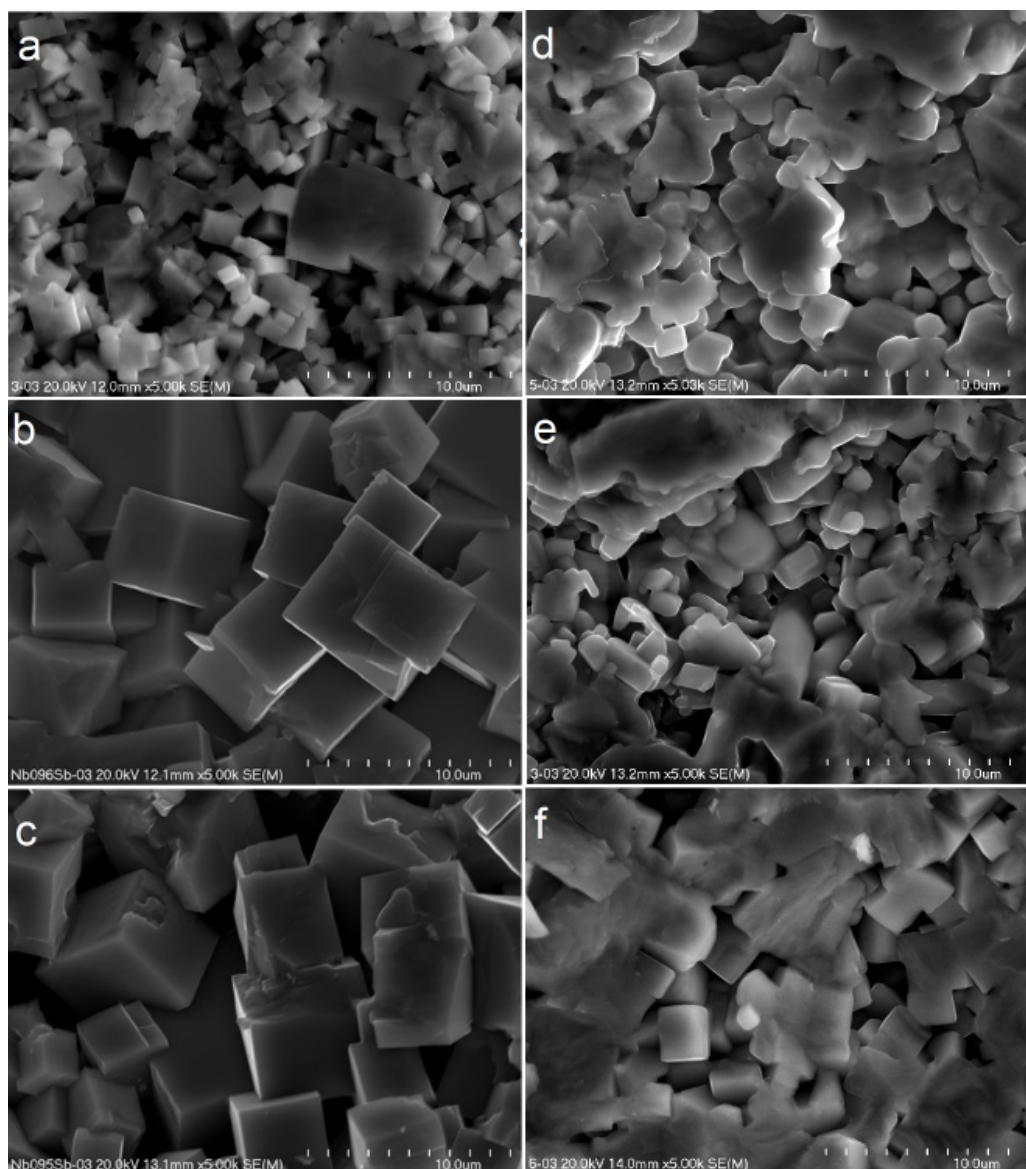


Fig. 1. SEM micrographs of the  $\text{Na}_{0.5}\text{K}_{0.5}\text{Nb}_{1-x}\text{Sb}_x\text{O}_3$  ( $x = 0.04$  (a),  $x = 0.05$  (b) and  $x = 0.06$  (c)) and  $\text{Na}_{0.5}\text{K}_{0.5}\text{Nb}_{1-x}\text{Sb}_x\text{O}_3 + 0.5 \text{ mol}\% \text{MnO}_2$  ( $x = 0.04$  (d),  $x = 0.05$  (e) and  $x = 0.06$  (f)) ceramics

(Fig. 1a-c). This suggests that Sb has no significant influence on the densification of these ceramics. In addition, these ceramics have some amount of pores. Addition of 0.5 mol% MnO<sub>2</sub> improves the densifications, e.g. amount of pores are less and grain size increases (Fig. 1d-f). However, sintering temperature of the ceramics decreases after 0.5 mol% MnO<sub>2</sub> addition (from 1140°C for NKNS to 1130°C for NKNS + 0.5 mol% MnO<sub>2</sub>).

Performed X-ray powder diffraction measurements showed that all studied samples at room temperature possess orthorhombic crystal system and only one single phase is visible without any impurities. Performed high temperature X-ray powder diffraction measurements showed that in studied temperature range two phase transitions are observed. Phase transition temperatures and temperature dependence of lattice parameters has been studied every 15° based on diffraction measurements performed

in 2θ range 44.0 to 47.5° where characteristic peak splitting is observed. Lattice parameters have been determined based on the position of measured diffraction peaks. Using FullProf program suite [5] precise lattice parameters were determined in orthorhombic, tetragonal and cubic phase in 2θ range 10 to 90°. First phase transition from orthorhombic to tetragonal crystal system is visible as combining of two orthorhombic diffraction peaks (200)<sub>O</sub> and (020)<sub>O</sub> into one tetragonal (002)<sub>T</sub> peak. During further increase of temperature second phase transition from tetragonal to cubic crystal system is observed also as combining of (200)<sub>T</sub> and (002)<sub>T</sub> diffraction peaks. In all samples the tetragonal to cubic phase transition is observed above the temperatures of 300°C. The temperature dependence of lattice parameters for selected samples has been shown in Fig. 2.

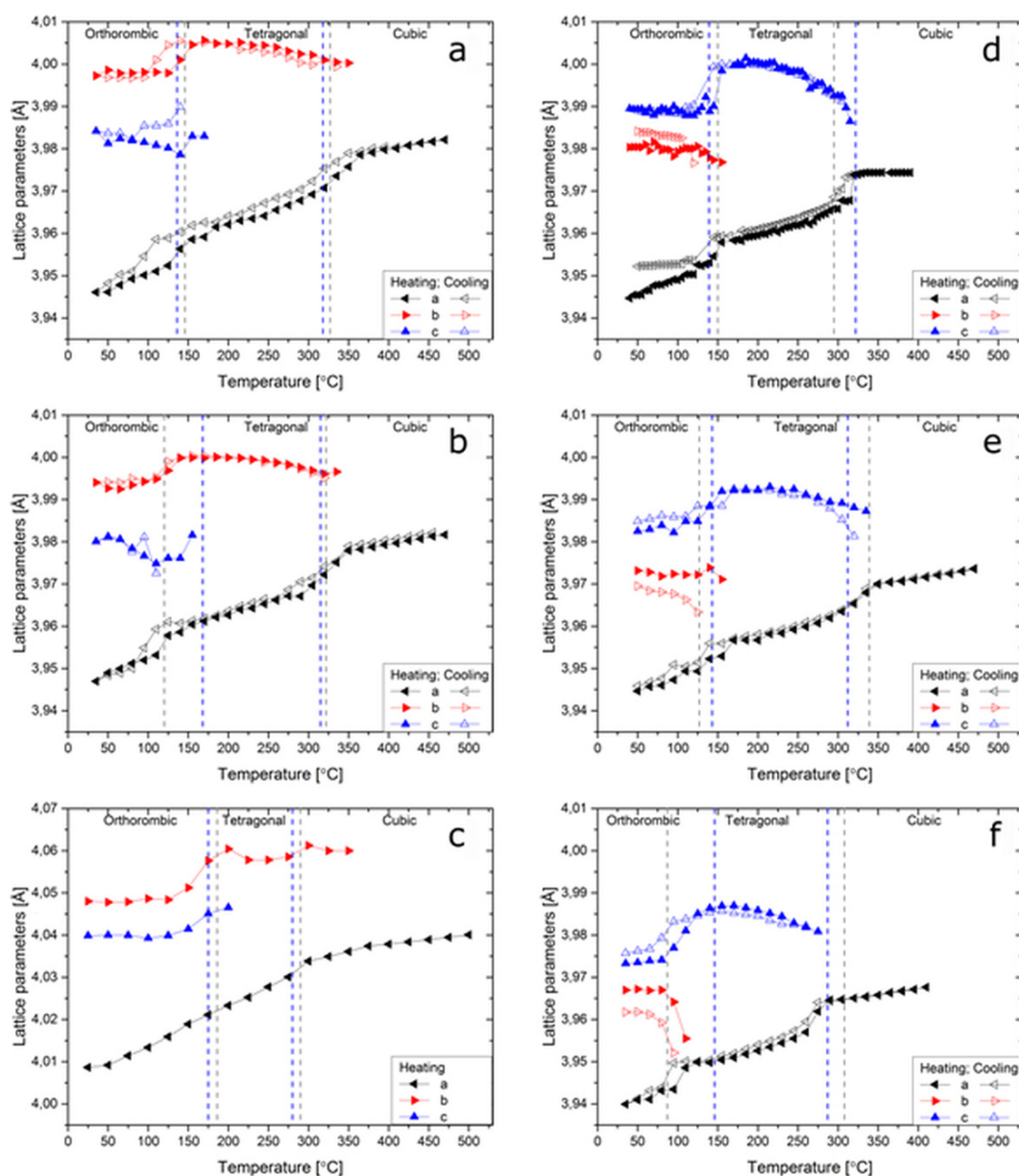


Fig. 2. Temperature dependence of lattice parameters of the  $\text{Na}_{0.5}\text{K}_{0.5}\text{Nb}_{1-x}\text{Sb}_x\text{O}_3$  ( $x = 0.04$  (a),  $x = 0.05$  (b) and  $x = 0.06$  (c)) and  $\text{Na}_{0.5}\text{K}_{0.5}\text{Nb}_{1-x}\text{Sb}_x\text{O}_3 + 0.5 \text{ mol\% MnO}_2$  ( $x = 0.04$  (d),  $x = 0.05$  (e) and  $x = 0.06$  (f)) ceramics during heating (filled symbols) and cooling (empty symbols) cycles determined from the X-ray diffraction measurements. Vertical lines correspond to the phase transition temperatures determined from the DSC (grey) and the dielectric (blue) measurements

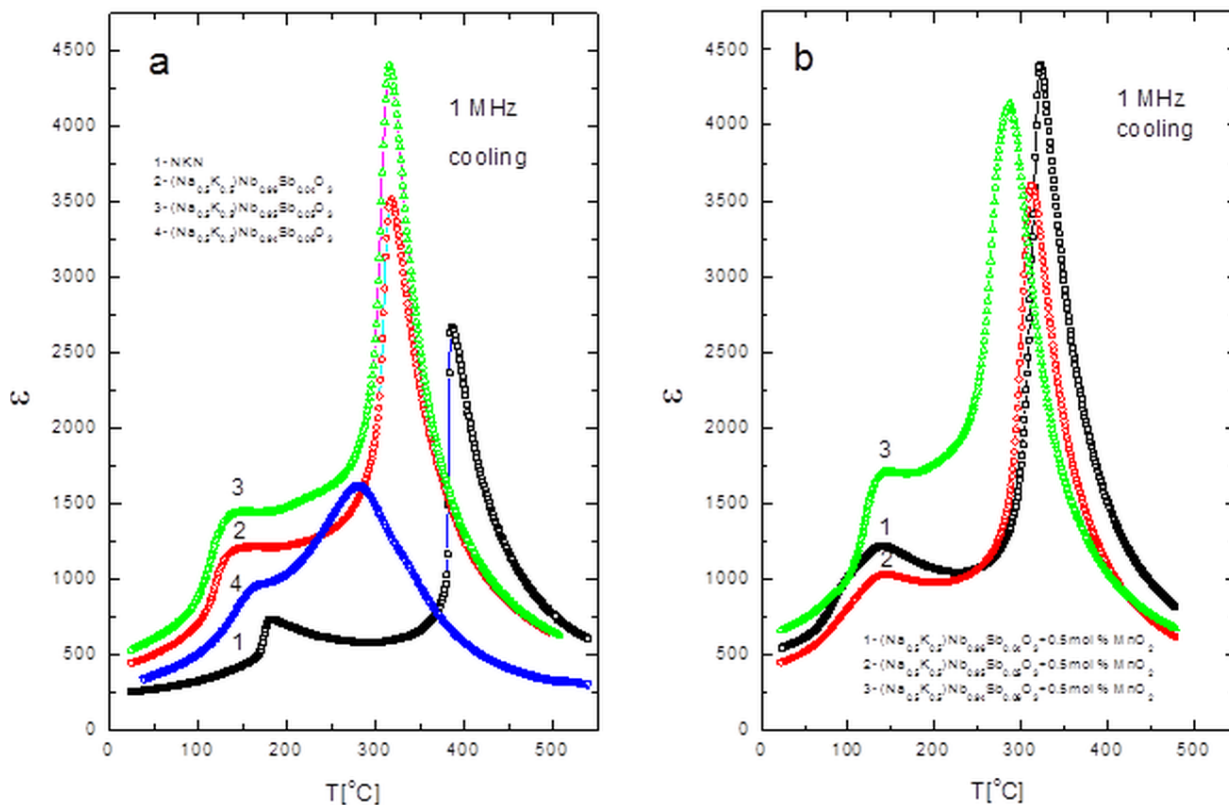


Fig. 3. Temperature dependence of electric permittivity of NKN and NKNS (a) and NKNS + 0.5mol%MnO<sub>2</sub> (b) ceramics

The temperature dependence of the electric permittivity of NKNS and Mn-doped NKNS ceramics measured at 1MHz is shown in Fig. 3. Pure NKN ceramics undergo a cubic-tetragonal phase transition at 388°C ( $T_c$ ) and tetragonal-orthorhombic one at 178°C ( $T_{T-O}$ ) [4], Table 1. Addition of Sb to NKN leads to decrease of both phase transitions temperatures and increases electric permittivity. Substitution of 0.5 mol%MnO<sub>2</sub> to previously Sb-doped NKN leads to further shifts of cubic-tetragonal phase transitions to lower temperature and tetragonal-orthorhombic one to higher temperature. Dielectric study results are in good accordance with X-ray results (Fig. 2).

Figure 4 shows the temperature dependence of heat flow for investigated ceramics on heating/cooling processes. The DSC curves exhibit distinct endothermic peaks on heating and exothermic peaks on cooling connected with tetragonal-cubic/cubic-tetragonal phase transition. DSC peaks connected with orthorhombic-tetragonal/tetragonal-orthorhombic phase transition are broad and worse visualized. In comparison to NKNS, the temperature of tetragonal-cubic and one of orthorhombic-tetragonal phase transition of NKNS + 0.5mol%MnO<sub>2</sub> is lower and higher, respectively, in agreement with dielectric measurements results (Table 1).

The room temperature Raman spectra of investigated ceramics are shown in Fig. 5. NKN has the orthorhombic C<sub>2v</sub> phase, which is represented by 12 Raman active optical modes: 4A<sub>1</sub> + 4B<sub>1</sub> + 3B<sub>2</sub> + A<sub>2</sub> [5]. The Raman spectra of pure NKN show four main peaks at about 63, 260, 612 and 857 cm<sup>-1</sup>. In addition, weak lines at about 137 and 450 cm<sup>-1</sup> and shoulders at right side of 63 cm<sup>-1</sup> and left side of 260 and 612 cm<sup>-1</sup> modes

exist. This spectrum is very similar to this reported in earlier paper [5]. Both, NKNS and NKNS + 0.5mol%MnO<sub>2</sub> are based on the original NKN and have similar phase structure at room temperature (see XRD results). In consequence, the Raman spectra of NKNS and NKNS + 0.5mol%MnO<sub>2</sub> are similar to that obtained for pure NKN. The changes of spectra after Mn-substituting of NKNS are mainly related to very small shift downwards of main lines, decrease of their intensity and small broadening. These changes are evidence of proper addition of Mn ion into the NKNS structure.

Figure 6 shows the P-E hysteresis loops of NKNS and NKNS + 0.5 mol%MnO<sub>2</sub> ceramics. All the specimens showed typical ferroelectric hysteresis loops. The remnant polarization increased after substitution both Sb to NKN and MnO<sub>2</sub> to NKNS, while coercive field seems to be unchanged.

TABLE 1

Phase transitions temperature from dielectric and DSC (in brackets) experiments (cooling) and room temperature piezoelectric properties of NKN, NKNS and NKNS + 0.5mol%MnO<sub>2</sub> ceramics

Item	T <sub>c</sub> (°C)	T <sub>T-O</sub> (°C)	d <sub>33</sub> (pC/N)	k <sub>33</sub> (%)
NKN	388 (385)	178 (175)	90	31
NKNS4	318 (327)	136 (146)	130	39
NKNS5	315 (322)	145 (120)	168	41
NKNS6	280 (290)	175 (186)	180	43
NKNS4 + 0.5mol%MnO <sub>2</sub>	322 (295)	139 (150)	140	40
NKNS5 + 0.5mol%MnO <sub>2</sub>	312 (339)	143 (127)	190	41
NKNS6 + 0.5mol%MnO <sub>2</sub>	287 (308)	146 (87)	192	43

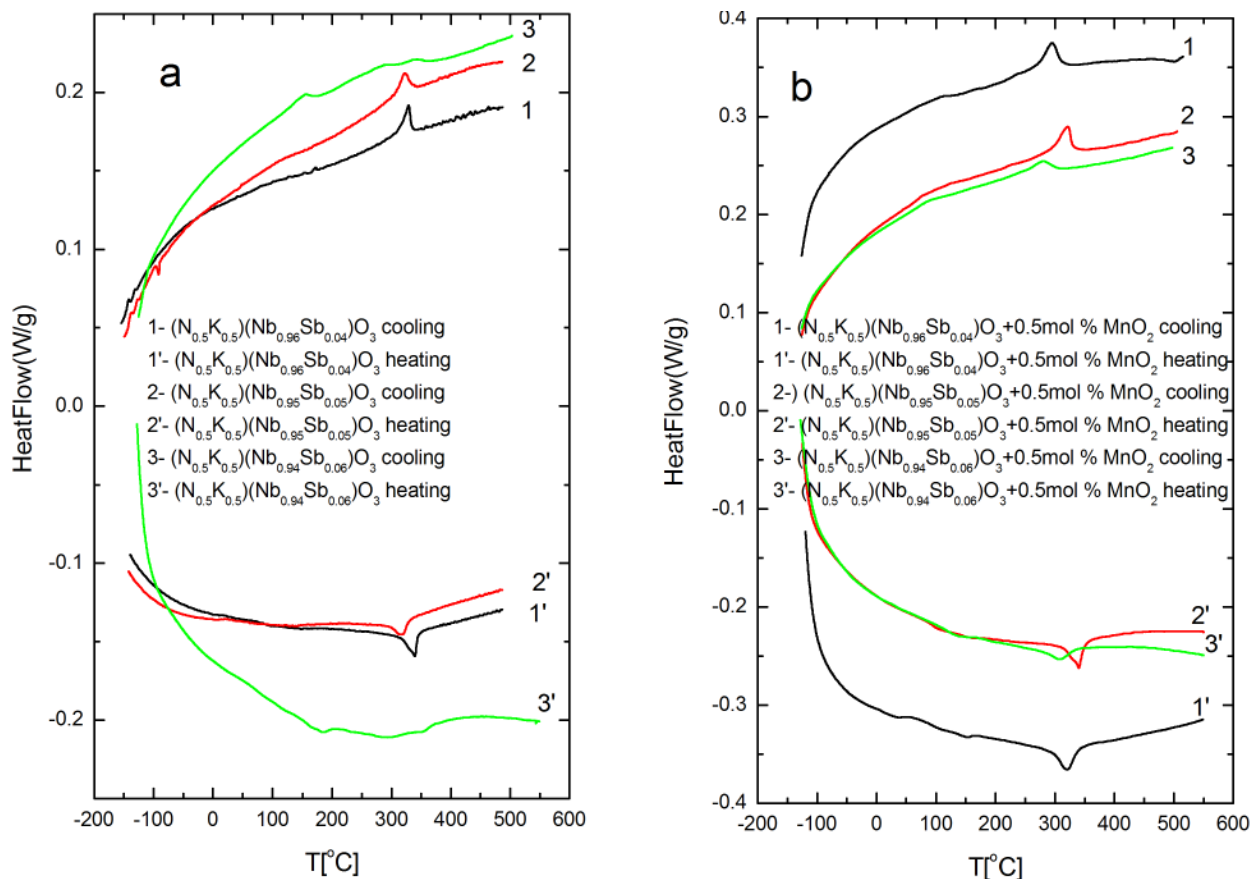


Fig. 4. Temperature dependence of the heat flow of NKNS (a) and NKNS + 0.5mol%MnO<sub>2</sub> (b) ceramics

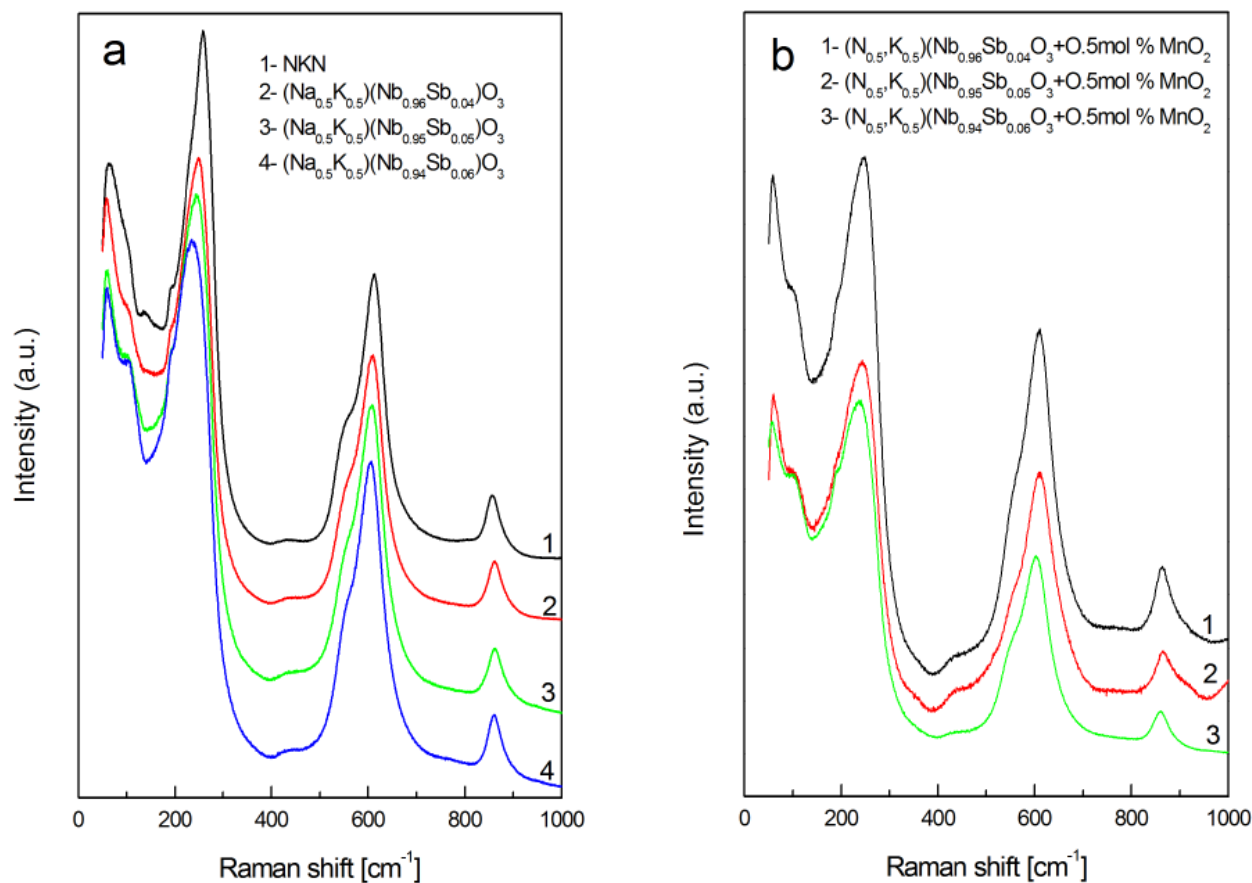


Fig. 5. Room temperature Raman spectra of NKN and NKNS (a) and NKNS + 0.5mol%MnO<sub>2</sub> (b) ceramics

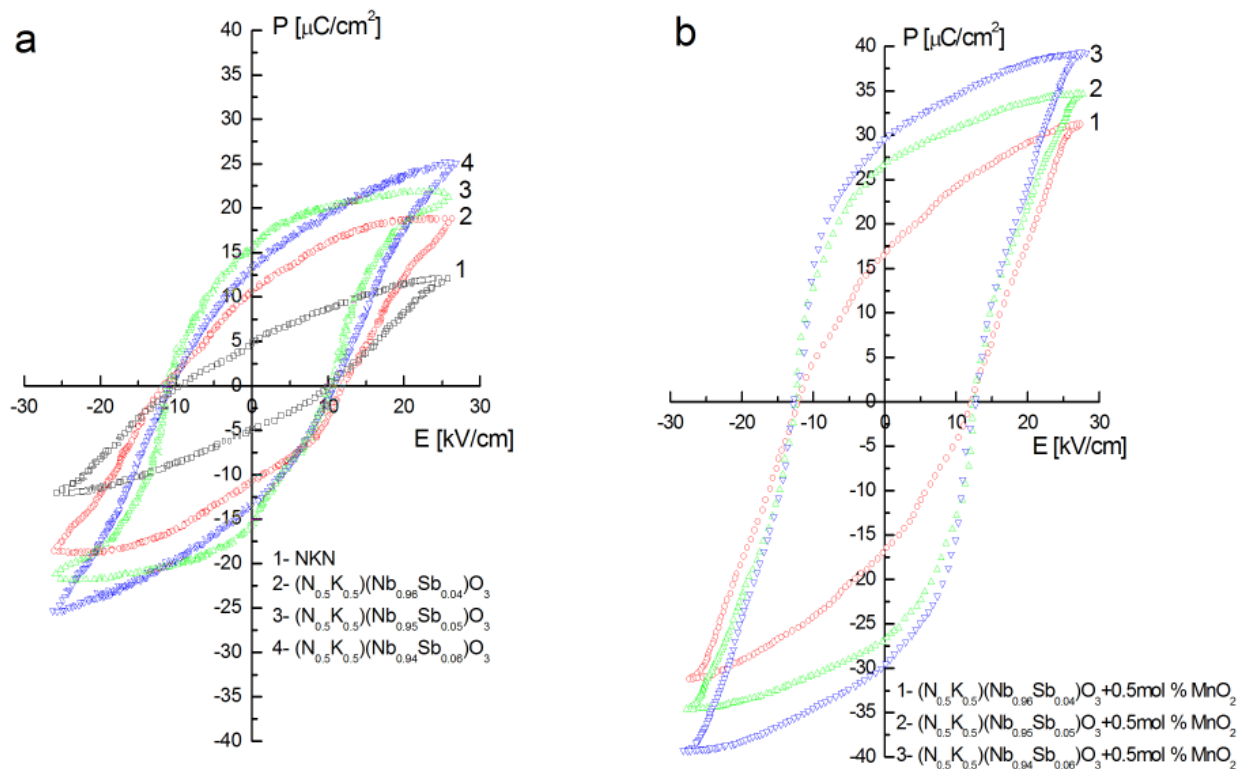


Fig. 6. Room temperature P-E hysteresis loops of the NKN and NKNS (a) and NKNS + 0.5 mol%MnO<sub>2</sub> (b) ceramics

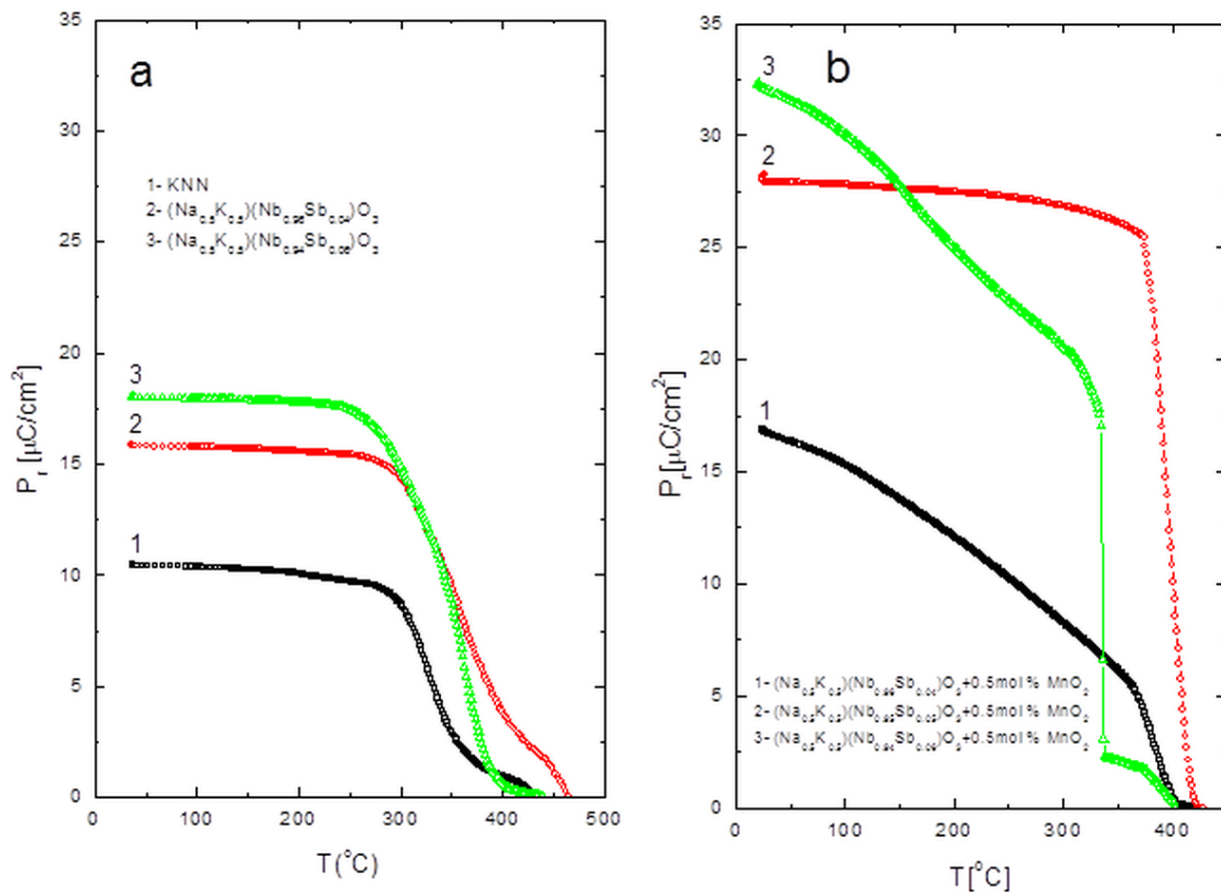


Fig. 7. Temperature dependence of the remnant polarization  $P_r$  (obtained from pyroelectric measurements) of NKN and NKNS (a) and NKNS + 0.5 mol%MnO<sub>2</sub> (b) ceramics

Figure 7 shows temperature dependence of remnant polarization  $P_r$  obtained from independent pyroelectric measurements of investigated ceramics showing very good agreement with hysteresis loops results (Fig. 6 for comparison).

The introductions of  $Sb^{5+}$  to NKN improve piezoelectric properties (Table 1).  $MnO_2$  doping NKNS leads to further improvement of its piezoelectric properties (Table 1).

Substitution of  $Sb^{5+}$  for  $Nb^{5+}$  can induce a stronger covalence due to difference of electronegativity (2.0 vs. 1.6). This substitution may give rise also to a larger off-centring of the cation as the ionic radius of  $Sb^{5+}$  (0.62 Å) is smaller than that of  $Nb^{5+}$  (0.69 Å). Both lead to improve the ferroelectric and piezoelectric properties. In addition,  $Sb^{5+}$ , similar to  $Pb^{2+}$  has a lone-pair (two electrons paired by their antiparallel spin in a filled sub-shell and not involved in chemical bonding). It is well known that Pb-containing compounds have very excellent ferroelectric and piezoelectric properties. However, enhancement of ferroelectric and piezoelectric properties of NKNS ceramics after addition of  $MnO_2$  can be mainly due to improvement of densification.

Manganese mainly exists in  $Mn^{2+}$  ( $r_{Mn^{2+}} = 0.80\text{Å}$ ) and  $Mn^{4+}$  ( $r_{Mn^{4+}} = 0.60\text{Å}$ ) stable states.

Considering  $Mn^{4+}$  as impurity centers, there is a good correspondence with  $Nb^{5+}$  in ionic radii and minimal difference in ionic charge. In this case impurity introduces excess negative charge (-e) into lattice. Corresponding charge compensator should have positive charge. It is well known, that the Schottky defect pairs (oxygen vacancy – cation vacancy) are typical for perovskites. So, oxygen vacancies ( $V_O$ ) could be considered as compensators for excess charge of  $Mn^{4+} \rightarrow Nb^{5+}$ .

If one assume  $Mn^{2+}$  as impurity centers, substitution  $Mn^{2+} \rightarrow Na^+$  ( $r_{Na^+} = 0.97\text{Å}$ ) or  $K^+$  ( $r_{K^+} = 0.81\text{Å}$ ) seems as probable variant. Here again one has charge difference, but in that case impurity introduces excess positive charge (+e) into the lattice. In such cases impurity suppresses arising of  $V_O$  and induces appearing of cation vacancies which compensate charge imbalance.

#### 4. Conclusions

The effect of Sb and  $MnO_2$  addition on microstructure and crystal structure, phase transitions and electric properties of NKN ceramics fabricated by conventional solid-state hot pressing technique was investigated. The ceramics can be well sintered at  $1100^\circ\text{C} \div 1140^\circ\text{C}$ . The results revealed that both Sb and Mn ions diffuse into NKN lattices and form a homogenous solid solution with perovskite structure of orthorhombic symmetry. The introduction of  $Sb^{5+}$  to NKN decreases the temperatures of cubic-tetragonal and tetragonal-orthorhombic phase transitions and improve ferroelectric and piezoelectric properties. The incorporation of Mn ion to NKNS leads to further decrease of cubic-tetragonal and increase of tetragonal-orthorhombic phase transitions and improve ferroelectric and piezoelectric properties. The results were discussed in term of difference in both ionic size and in electronegativity of  $Nb^{5+}$  and  $Sb^{5+}$  and improvement of densification after  $MnO_2$  doping.

#### REFERENCES

- [1] Y. Saito, H. Takao, T. Nonoyama, K. Takatori, T. Homma, T. Nagaya, M. Nakamura, *Nature* **432**, 84-87 (2004).
- [2] J. Acker, H. Kungl, M.J. Hoffmann, *J. Am. Cer. Soc.* **93**, 1270-1281 (2010).
- [3] J. Rodriguez-Carvajal, *Physica B* **192**, 55-69 (1993).
- [4] J. Suchanicz, I. Faszczowy, D. Sitko, J. Kusz, M. Zubko, P. Jeleń, M. Antonova, A. Sternberg, W. Hofmeister, *Phase Transitions* **87**, 992-1001 (2014).
- [5] E. Buixaderas, D. Nuzhnyy, I. Gregora, S. Kamba, M. Berta, B. Malic, M. Kosec, *IEEE Transactions on Ultrasonics, Ferroelectric and Frequency Control* **56**, 1843-1849 (2009).